Journal of Magnetic Resonance 194 (2008) 16–24

Contents lists available at ScienceDirect

Journal of Magnetic Resonance

journal homepage: www.elsevier.com/locate/jmr

Residual methyl protonation in perdeuterated proteins for multi-dimensional correlation experiments in MAS solid-state NMR spectroscopy

Vipin Agarwal [a], Bernd Reif [a,b,*]

[a] Leibniz-Forschungsinstitut für Molekulare Pharmakologie (FMP), Campus Berlin-Buch, Robert-Rössle-Strase, 10, D-13125 Berlin, Germany
[b] Charité Universitätsmedizin, D-10115 Berlin, Germany

ARTICLE INFO

Article history:
Received 12 February 2008
Available online 20 June 2008

Keywords:
MAS solid-state NMR
Magic angle spinning
Perdeuteration
Microcrystalline proteins
TOBSY
TOCSY

ABSTRACT

NMR studies involving perdeuterated proteins focus in general on exchangeable amide protons. However, non-exchangeable sites contain as well a small amount of protons as the employed precursors for protein biosynthesis are not completely proton depleted. The degree of methyl group protonation is in the order of 9% for CD_2H using >97% deuterium enriched glucose. We show in this manuscript that this small amount of residual protonation is sufficient to perform 2D and 3D MAS solid-state NMR experiments. In particular, we suggest a HCCH-TOBSY type experiment which we successfully employ to assign the methyl resonances in aliphatic side chains in a perdeuterated sample of the SH3 domain of chicken α-spectrin.

1. Introduction

Solid-state NMR spectroscopy has rapidly progressed over the last decade. However, the standards achieved for solution-state NMR are still remote mostly due to the broad resonances obtained for most of the investigated samples and the low sensitivity due to low γ nucleus detection. Currently, there are three general ways to achieve proton line narrowing in MAS solid-state NMR: The first approach is based on quenching the proton dipolar bath by spinning the sample at very high rotation frequencies around the magic angle. Improvements in MAS technology have made high frequency (~70 kHz) sample spinning possible [1–3]. Typical proton line widths are in the order of 300 Hz. A second, spectroscopic approach involves design of windowed homonuclear decoupling sequences which allow to achieve proton line widths in the order of 170–200 Hz (taking the scaling factor of the multiple pulse sequence into account) [4–8]. Third, the chemical approach involves dilution of the strongly coupled proton spin systems by deuteration. We and others could demonstrate that replacement of non-exchangeable protons by deuterons allows to significantly improve the resolution of the remaining exchangeable amide protons [9–15]. In order to increase proton resolution even further, we suggested to prepare samples using 90% D_2O in the crystallization buffer [16,17]. This way, typical ^1H and ^{15}N line widths in the order of 25 and 15 Hz, respectively, are achievable at rotation frequencies of around 24 kHz. In comparison to samples which were re-crystallized from 100% H_2O, a gain in resolution of a factor of 5 and 3 for the ^1H and ^{15}N dimension is observed, respectively. As the integral spectral area of the individual cross peaks is decreased accordingly by a factor of 15, sensitivity is effectively not compromised even though only 10% of the maximum equilibrium magnetization is employed in all experiments. A further decrease in experimental time can be achieved if the sample is doped with complexed paramagnetic ions which results in a reduction of the experimental time of up to a factor of 15 without compromising spectral quality [18]. This particular labeling scheme enables the accurate measurement of $^{15}NT_1$ [19] and T_2 related relaxation parameters by the determination of ^{15}N CSA/^1H-^{15}N dipole cross-correlated relaxation [20,21]. In addition, deuterons can serve as local probes to access side chain mobility in uniformly labeled proteins by determination of ^2H relaxation and line shape properties [22,23]. Furthermore, comparison of solution-state and solid-state NMR dynamics might be a promising way to better understand protein molecular motion in general [24,25]. Focussing on non-exchangeable sites and working with specifically labeled precursors of amino acid biosynthesis, the complete Boltzmann magnetization can be retained resulting in an additional 5-fold gain in sensitivity [26]. Recently, we have used 3-[66%-^2H,^{13}C] pyruvate as a precursor in protein biosynthesis to generate differentially protonated methyl groups (CH_3, CDH_2, CD_2H and CD_3) [27]. We found that the CD_2H isotopomer yielded the best dispersed proton spectrum.

In this article, we suggest to employ the residual protonation in aliphatic side chains of otherwise perdeuterated proteins to per-

* Corresponding author. Address: Leibniz-Forschungsinstitut für Molekulare Pharmakologie (FMP), Campus Berlin-Buch, Robert-Rössle-Strase, 10, D-13125 Berlin, Germany. Fax: +49 30 94793 191.
E-mail address: reif@fmp-berlin.de (B. Reif).

1090-7807/$ - see front matter © 2008 Elsevier Inc. All rights reserved.
doi:10.1016/j.jmr.2008.05.021

form multi-dimensional NMR experiments. We estimate the approximate degree of protonation in a methyl group and show that proton-detected 3D HCCH-TOBSY type experiments can be performed with high-sensitivity at this low degree of protonation.

2. Materials and methods

2.1. Sample preparation

An u-[^{2}H,^{13}C,^{15}N] isotopically enriched chicken α-spectrin SH3 sample was used for all experiments described in this manuscript. The protein was expressed, purified and re-crystallized as reported previously [16].

2.2. NMR spectroscopy

All experiments were collected on a Bruker Avance NMR spectrometer operating at a proton Larmor frequency of 600.13 MHz, equipped with a standard 3.2 mm ^{1}H/X/Y broadband triple-resonance probe. The channels X and Y were tuned to carbon and deuterium, respectively. The MAS frequency was set to 20 kHz in all experiments. The nominal probe temperature was adjusted to 2 °C. The effective sample temperature is higher due to MAS induced heating. We estimate the actual sample temperature to be in the order of 18 °C based on the temperature sensitive hydroxyl resonance of methanol which was used as an external standard.

In the HCCH-TOBSY experiment (Fig. 1), magnetization is transferred first from the methyl protons to carbons using a refocused INEPT element. In the second step of the preparation period, an adiabatic TOBSY sequence [28,30–32] (^{13}C scalar mixing) distributes magnetization along the carbon side chain. TOBSY mixing was achieved by applying a train of 180° adiabatic tanhtan pulses. The product of the adiabatic pulse bandwidth and the pulse length was 62. The ^{13}C RF field strength was adjusted to 55 kHz for ^{13}C,^{13}C scalar mixing. After the preparation period, carbon magnetization is frequency labeled in ω_1. The back-transfer involves an adiabatic TOBSY sequence of equal duration and a second refocussed INEPT element to transfer magnetization back to methyl protons for detection. Due to the dilute proton bath, no high power decoupling is required. Asynchronous application of adiabatic 180° pulses with respect to the rotor cycle prevents recoupling of the homonuclear ^{13}C,^{13}C dipolar couplings. To refocus the ^{1}H,^{13}C scalar couplings during t_1 and t_2, π pulses are applied on the proton channel in the center of the evolution period, while broad band scalar decoupling (WALTZ-16) is used to decouple protons from carbons in the direct dimension. Similarly, WALTZ-16 is applied on the ^{2}H channel in t_1, t_2 and during acquisition to remove ^{2}H,^{13}C scalar couplings. Deuterium decoupling is essential to achieve high-resolution along the ^{13}C dimension [27]. The spectral widths were set to 33.3, 22 and 69 ppm in ω_3, ω_2 and ω_1, respectively, with the ^{13}C transmitter frequency being centered at 20 ppm. Prior to the t_1 evolution period, the carbon offset was shifted to 41.4 ppm in order to avoid folding of the aliphatic resonances in the ω_1 dimension. To record the 3D data set, 128 and 64 points were acquired in the t_1 and t_2 dimensions, respectively, accumulating 16 transients in each FID. The recycle delay was set to 2.5 s. The total experimental time amounted to approximately 91 h. All data were processed using the software Topspin (Bruker). A cosine squared bell function was used for apodization. 2048, 512 and 1024 points were used for zero filling in the ω_3, ω_2 and ω_1 dimension, respectively. The analysis and the assignment of the 3D spectrum was carried out in SPARKY [33].

3. Results and discussion

3.1. Residual protonation at non-exchangeable sites in perdeuterated proteins

Methods for the preparation of uniformly deuterated proteins have been well worked out in the past [34]. Usually, perdeuterated proteins are employed to reduce homo- and heteronuclear ^{1}H,^{1}H and ^{1}H,^{13}C dipolar interactions, and to achieve favorable spectral properties of the remaining (mostly exchangeable) proton and carbon resonances. The commercially available ^{2}H,^{13}C labeled glucose and D_2O allow to achieve this goal only to a certain extent, as the chemicals are available with a degree of enrichment which is in the order of 97% and 99%, respectively. In addition to exchangeable protons, a small amount of protons should therefore be left on the aliphatic side chains. Fig. 2A represents the 1D proton spectrum of the perdeuterated α-spectrin SH3 domain re-crystallized in a buffer containing H_2O and D_2O at a ratio of 1:9. We find significant intensities for resonances in the methyl region of the spectrum (approximately 2–3 times smaller compared to the resonances in the proton amide region). These are due to the residual protonation of the methyl groups. We refer to this residual protonation at non-exchangeable sites in biosynthetically expressed, uniformly deuterated proteins as "^{1}*H At N*atural *A*bundance In ^{2}*H* Proteins" (HANAH). In this scheme, protons are randomly distributed across the protein, implying that the proton network is sufficiently dilute to detect protons in the solid-state with high-resolution and sensitivity.

In order to estimate the exact concentration of the CD_2H moieties in the sample, we measure the relative peak intensity of the two isotopomers [CD_2H/CD_3] using a ^{13}C one pulse experiment (Fig. 2B). In comparison to CD_3, the CD_2H isotopomer is ca. 0.3 ppm downfield shifted [35]. For I30δ, a strong peak originates from the dominant CD_3 group, while satellite peaks due to the CD_2H isotopomer appear at the base of the CD_3 resonance. The spectra were recorded in the absence of proton scalar decoupling to facilitate the separation of the two species. As u-^{13}C glucose was used as carbon source, carbon resonances are split into doublets due to the ^{13}C,^{13}C one bond scalar coupling. Peaks stemming

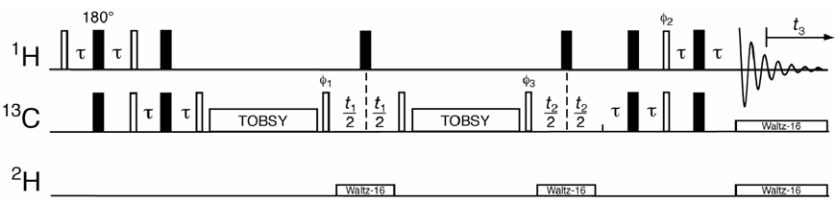

Fig. 1. ^{1}H detected 3D HCCH-TOBSY pulse scheme. Open and solid bars represent $\pi/2$ and π pulses, respectively. The MAS frequency was adjusted to 20 kHz. A RF field strength of 60 and 43 kHz was used on the ^{1}H and ^{13}C channel, respectively. An adiabatic version of TOBSY [28] was used for ^{13}C,^{13}C mixing with 40 μs, 180° tanhtan pulses. A P5m4 phase cycle [28,29] was employed to generate isotropic scalar mixing. TOBSY mixing was applied for a duration of 11.2 ms. The duration of τ was set to 1.8 ms corresponding to $1/4^{*}\,{}^{1}J_{CH}$. A RF field strength of 1.5–2.5 kHz on both the ^{13}C and ^{2}H channels was applied for WALTZ-16 decoupling. The phase cycle $\phi_1 = +y, -y$, $\phi_2 = +x, +x, -x, -x$, $\phi_3 = 4(+y), 4(-y)$ and $\phi_{rec} = +x, -x, -x, +x, -x, +x, +x, -x$ was employed. The ^{1}H and ^{2}H carrier was positioned on the water and D_2O resonance, respectively. Quadrature detection in ω_1 and ω_2 is achieved using TPPI.

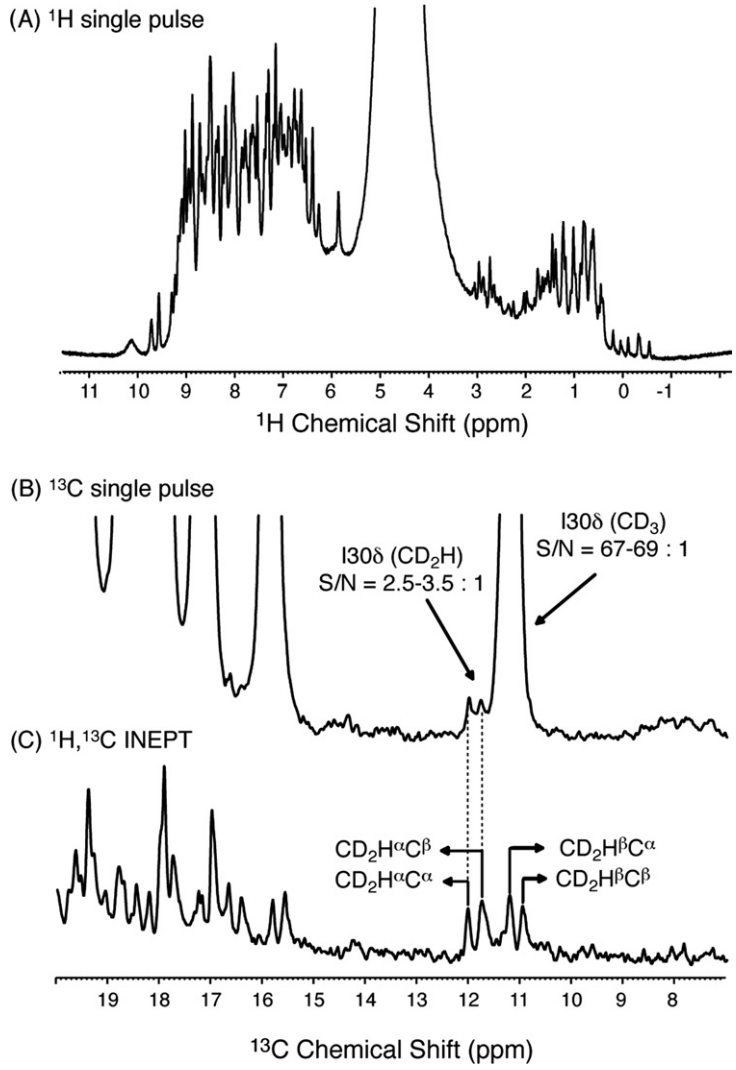

Fig. 2. (A) ^{1}H spectrum of the chicken α-spectrin SH3 domain. The deuterated protein (grown on [> 97%-^{2}H, 99%-^{13}C] labeled glucose, ^{15}N ammonium chloride) was recrystallized from a buffer solution containing D_2O and H_2O at a ratio of 9:1. The ^{13}C spectrum of the protein acquired using (B) direct ^{13}C excitation, and (C) ^{1}H,^{13}C INEPT to select for proton carbon pairs. WALTZ-16 was used to remove one bond ^{2}H,^{13}C scalar couplings. Couplings to protons were allowed to evolve to facilitate the assignment of the spin system.

from the spin states $CD_2H^{\alpha}C^{\alpha}$ and $CD_2H^{\alpha}C^{\beta}$ are well resolved, while peaks due to $CD_2H^{\beta}C^{\alpha}$ and $CD_2H^{\beta}C^{\beta}$ states are buried under the CD_3 peak. For comparison, Fig. 2C represents a ^{13}C spectrum that was acquired using ^{1}H,^{13}C INEPT for magnetization transfer from protons to carbons. Again, the spectrum was recorded without proton scalar decoupling. Clearly, a doublet of doublets is observable for the I30δ resonance which is due to $^{1}J_{CH}$ and $^{1}J_{CC}$. Integrating the CD_3 and CD_2H resonances for I30δ (Fig. 2B), we find an enrichment of the CD_2H isotopomer in the order of (8.8 ± 1.6)%.

3.2. 2D $^{1}H,^{13}C$ correlations using scalar and dipolar couplings for transfer: identification of methyl groups located in rigid and mobile segments of the protein

The residual protonation of 8.8% is sufficient to perform high sensitivity 2D ^{1}H,^{13}C correlation experiments. Fig. 3 represents two ^{1}H,^{13}C correlations using scalar (black) and dipolar (red) couplings for heteronuclear magnetization transfer. We find that the HMQC spectrum yields additional resonances originating from methionine-1 and threonine-4. We observe that the sensitivity of the HMQC is approximately three times higher compared to the double CP experiment. This is due to the limited sensitivity of the heteronuclear Hartmann–Hahn transfer in the solid-state. By comparing the sensitivity of a proton-detected single pulse experiment to the sensitivity of a proton-detected double CP experiment, we find that the transfer efficiency for a single CP step is in the order of 55%. Values closer to the theoretical limit of 0.73 are difficult to achieve at high rotation frequencies [36]. At high MAS rotation frequencies (40 kHz), ^{1}H,^{13}C correlation experiments become possible even in the absence of deuteration [3]. However, the intrinsic resolution in protonated samples is still significantly decreased.

Dipolar coupling mediated experiments retain resonances from rigid segments of the protein, while the mobile parts can be identified using solution-state NMR type pulse schemes [37,38]. In protonated solids, scalar and dipolar experiments yield complementary information. For extensively diluted spin systems, however, scalar coupling mediated experiments supplement the dipolar based experiments, as all resonances should be retained during INEPT type transfer steps. This property could be used for spectral editing in larger spin systems.

3.3. 3D HCCH-TOBSY correlation experiment

Even though this degree of protonation seems rather meager, it is sufficient to perform multi-dimensional spectroscopy. Fig. 1 represents the pulse scheme that we suggest to obtain methyl group

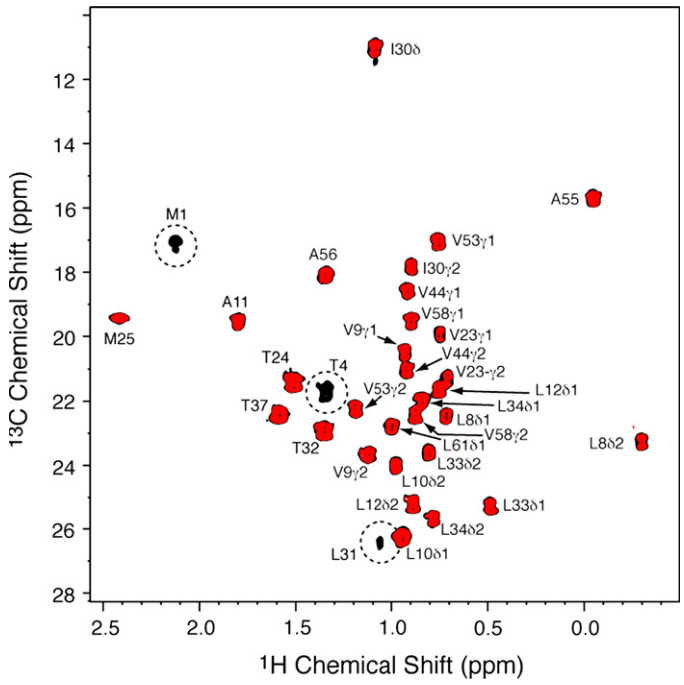

Fig. 3. $^{1}H,^{13}C$ correlation spectrum for the extensively deuterated SH3 domain at ^{1}H "natural abundance". The HMQC and the double CP experiment are drawn in black and red, respectively. The experiments were recorded at an effective sample temperature of 18 °C.

resonance assignments with detection on the proton in a CD_2H moiety. The assignments of the methyl groups is based on the knowledge of the Cα and Cβ chemical shifts which are obtained independently. The description of the pulse sequence is given in the experimental section. The sequence is very similar to the HCCH-TOCSY experiment suggested by Bax and co-workers [39]. In contrast to the original experiment, we aim to transfer magnetization out-and-back. Similar experiments using relay steps for magnetization transfer were suggested by Kay and co-workers in solution-state NMR spectroscopy [40,41]. Recently, scalar relay transfer elements have been successfully implemented by Mueller and co-workers to obtain $^{13}C,^{13}C$ connectivities for backbone assignments of a crystalline protein in MAS solid-state NMR experiments [42,43]. We have chosen TOBSY for mixing as this sequence allows to distribute the magnetization among many carbon spins independent of the side chain topology, without having to adjust the experiment to an individual amino acid. Fig. 4A shows strip plots from the 3D HCCH-TOBSY data set for alanine and threonine residues of the α-spectrin SH3 domain. In case of alanine, three frequencies ($^{13}CO,^{13}C\alpha$ and $^{13}C_\beta$) can be used to identify the respective spin system. In most cases, magnetization can be transferred as far as to the carbonyl carbon. The carbonyl resonances are folded back into the aliphatic region of the spectrum and appear with negative intensity. Similarly for threonine methyls, three correlations are observable. For methionine only the auto-correlation peak is visible (data not shown).

Fig. 4B shows HCCH-TOBSY strip plots for valine residues of the α-spectrin SH3 domain. In contrast to the alanine and threonine correlations, valines show predominantly contacts between the two methyl groups. Surprisingly, the two bond correlation between the two methyls is observable while the one bond correlation to Cβ is absent. Similarly, leucine shows strong two bond correlations between the two methyl groups while the one bond correlation to Cγ appears to be weak (data not shown). The same is true for isoleucine. We find an intense correlation between Ile-δ and Cγ1, while correlations to other carbons are missing. Isoleucine Cγ-2 does not show any correlation. In order to find out if these magnetization transfer characteristics are specific for TOBSY, we recorded the same experiment using RFDR for mixing (mixing time: 2 ms). There, only one bond methyl Cβ correlations are observed (red contours in Fig. 4B). To better understand the mixing time dependence of the magnetization buildup dynamics on an individual carbon spin, we carried out SIMPSON [44] simulations for all methyl bearing side chains (see Appendix). We find good agreement between the simulation and the experimental results. Generally, we observe all correlations that have more than 20% intensity in our simulation at a TOBSY mixing time of 11.2 ms. In order to demonstrate that the experimental implementation of the 3D HCCH-TOBSY experiments works well for all methyl bearing amino acids, we recorded 2Ds at various mixing times frequency-labeled in (f_1, f_3) in the pulse scheme described in Fig. 1, using the triply labeled dipeptide NAc-Val-Leu-OH as a model system (see Appendix). There, in fact, all possible correlations up to the carbonyl resonance are observable.

To summarize, complete side chain correlations for methyl bearing residues can be obtained in a 3D HCCH-TOBSY experiment if the optimal mixing time is chosen. At this point, we are limited in sensitivity as we employ the HANAH approach to yield a proton dilute solid-state NMR sample. The sensitivity of the experiment could be enhanced by several means: (1) An additional factor of approximately 13 in sensitivity can be gained if specifically labeled precursors, such as α-ketoisovalerate and/or α-ketobutyrate are employed as supplement in the growth medium during biosynthesis. (2) A majority of the experimental time goes into recycle delay (2.5 s) because of the relatively long spin lattice relaxation times of the methyl protons. Use of Cu(II)-EDTA doped samples can reduce the recycle delay to less than a second yielding an additional factor of three reduction in measurement time.

4. Conclusion

We could show in this manuscript that proton-detected MAS solid-state NMR experiments involving protons at natural abundance in perdeuterated and uniformly ^{13}C enriched crystalline proteins can be accomplished at relatively high-sensitivity. We observe resonance line widths which are in the order of 20–30 and 7–12 Hz for methyl protons and carbons, respectively. We could demonstrate that a 3D HCCH-TOBSY experiments can be applied to assign methyl proton and carbon resonances. We expect that this experiment will be of importance in the context of the structural analysis of the side chains of amyloidogenic peptides as well as for membrane proteins.

Acknowledgments

This research was supported by the Leibniz-Gemeinschaft and the DFG (Re1435, SFB449, SFB740, FOR475). We thank Kristina Rehbein and Anne Diehl for providing the triply labeled SH3 sample. We are grateful to Prof. Dr. Steffen Glaser, TU München, for stimulating discussions and first simulations. We acknowledge Dr. Thomas Vosegaard, University Aarhus, for providing SIMPSON patch files to directly read in BRUKER shapes.

Appendix

We find experimentally, that the TOBSY mixing scheme works very well for out-and-back mixing involving three to four spins like alanine and threonine. However, transfer efficiencies are much reduced for branched side chains like valine, leucine and isoleucine. We present simulations in this appendix which

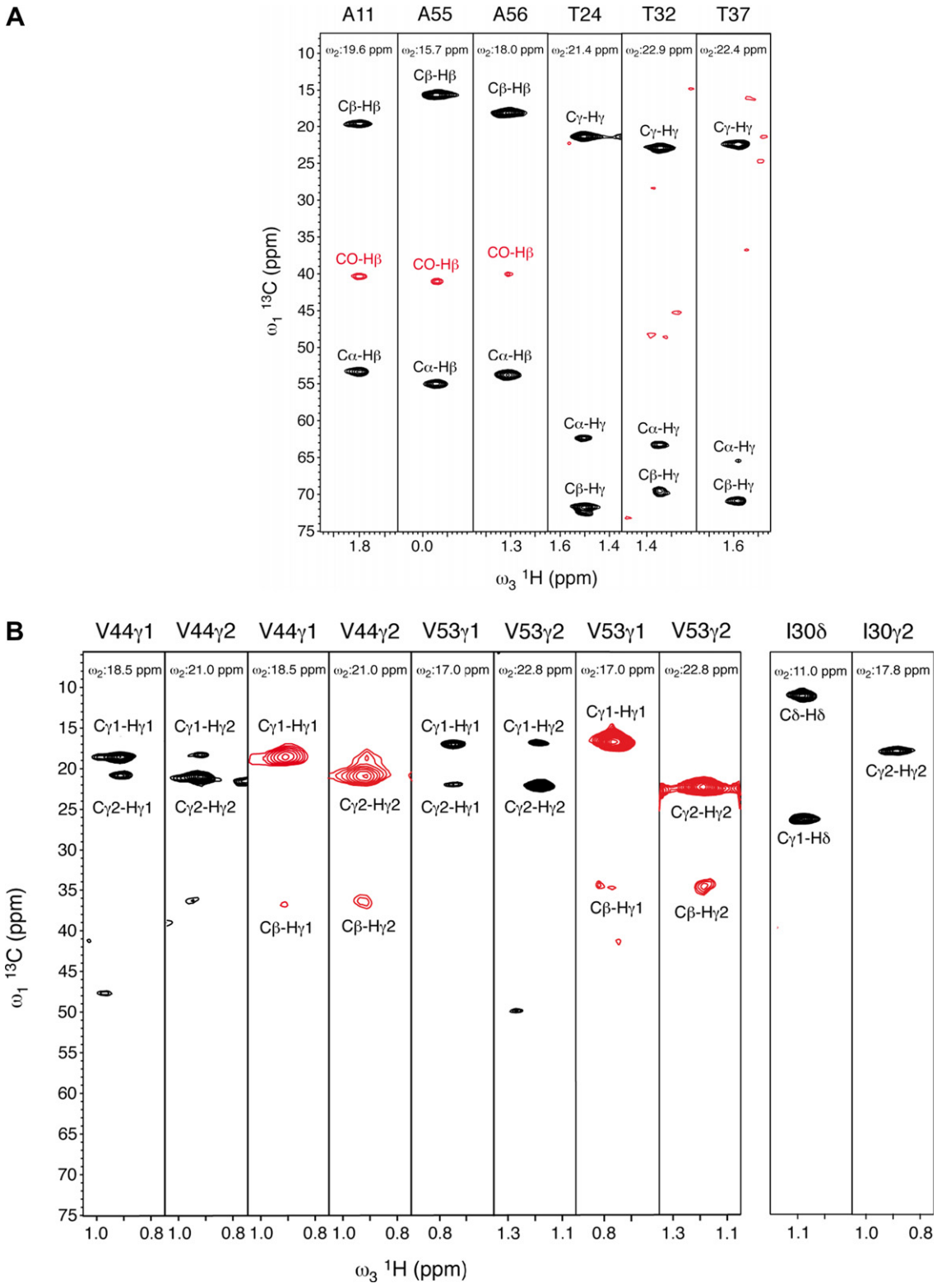

Fig. 4. Strip plots extracted from the 3D HCCH-TOBSY spectrum for various residues of the u-[^{2}H,^{15}N,^{13}C] α-spectrin SH3 domain. The TOBSY ^{13}C,^{13}C mixing time was adjusted to 11.2 ms. Panel (A) focuses on alanine and threonine residues, whereas (B) represents different valine spin systems. For spectra draw in black contours, the scalar TOBSY mixing sequence was employed, whereas RFDR was used in the spectra that are drawn with red contour lines.

yield the ideal mixing time for an individual spin system. In addition, we repeated the experiments using the triply labeled model peptide NAc-Val-Leu-OH and show that the suggested sequence works well in case the experimental sensitivity is not limiting.

Simulations of TOBSY transfer efficiencies in various spin systems

Several through bond transfer sequences have been suggested for magnetization transfer in rotating solids [28,30,32,45]. The simultaneous presence of scalar and dipolar couplings complicates

the transfer dynamics. The time dependent Hamiltonian of a system of two coupled homonuclear spin-1/2 nuclei can be written as

$$H(t) = H_{CS}(t) + H_J + H_D(t) \quad (1)$$

with

$$H_{CS}(t) = \delta_1(t)I_{1z} + \delta_2(t)I_{2z}$$
$$H_J = 2\pi J I_{1z}I_{2z}$$
$$H_D(t) = d_{12}(t)\{2I_{1z}I_{2z} - I_{1x}I_{2x} - I_{1y}I_{2y}\}$$

For an ideal through bond transfer, the first and third term in Eq. (1) should be zero, such that the Hamiltonian only depends on scalar couplings. In order to evaluate the efficiency of the pulse sequence under a number of different parameters such as chemical shift difference, irradiation frequency and the explicit form of an experimentally implemented shape, we simulated the performance of the mixing sequence using SIMPSON [44]. We employed an adiabatic non-rotor synchronized tanh shape [28] for $^{13}C,^{13}C$ mixing. The tanh 180° pulse was applied for a duration of 0.8 * τ_R (τ_R = rotor period) using p5m4 phase cycling. Naively, a train of 180° pulses should refocus the chemical shift, and application of non-rotor synchronous pulses should average out dipolar couplings. In total, this should yield an ideal isotropic behavior. We first examine the transfer profile for a two spin system, and extend this later to the carbon spin system of methyl bearing amino acids. In all simulations, magnetization transfers are assumed to be one-way transfers. The out-and-back scheme of the pulse sequence is not taken into account.

Definition of the mixing sequence in SIMPSON

The experimentally used shape file was directly read into SIMPSON. The adiabatic tanh shape was generated using the Bruker shape tool package available within XWINNMR. The same numerical shape was used for experiments and simulation. The product of pulse bandwidth and pulse length was set to 62. The shape consists of 100 steps of equal duration with variable amplitude and phase. All simulations were carried out at 20 kHz MAS, using a ^{13}C rf field of 60 kHz. The proton Larmor frequency was set to 600 MHz. Five gamma angles were employed in the par section. To obtain each transfer profile, 30 crystallites were averaged (using the internal SIMPSON crystallite file rep30).

Transfer characteristics for a two spin system

We evaluate the performance of the above described TOBSY sequence for a two spin system. Only the first spin is longitudinally polarized before the mixing sequence. Fig. 5A shows the build up of intensity on the spin 2 as a function of the chemical shift difference between the two (scalar and dipolar) coupled spins. The

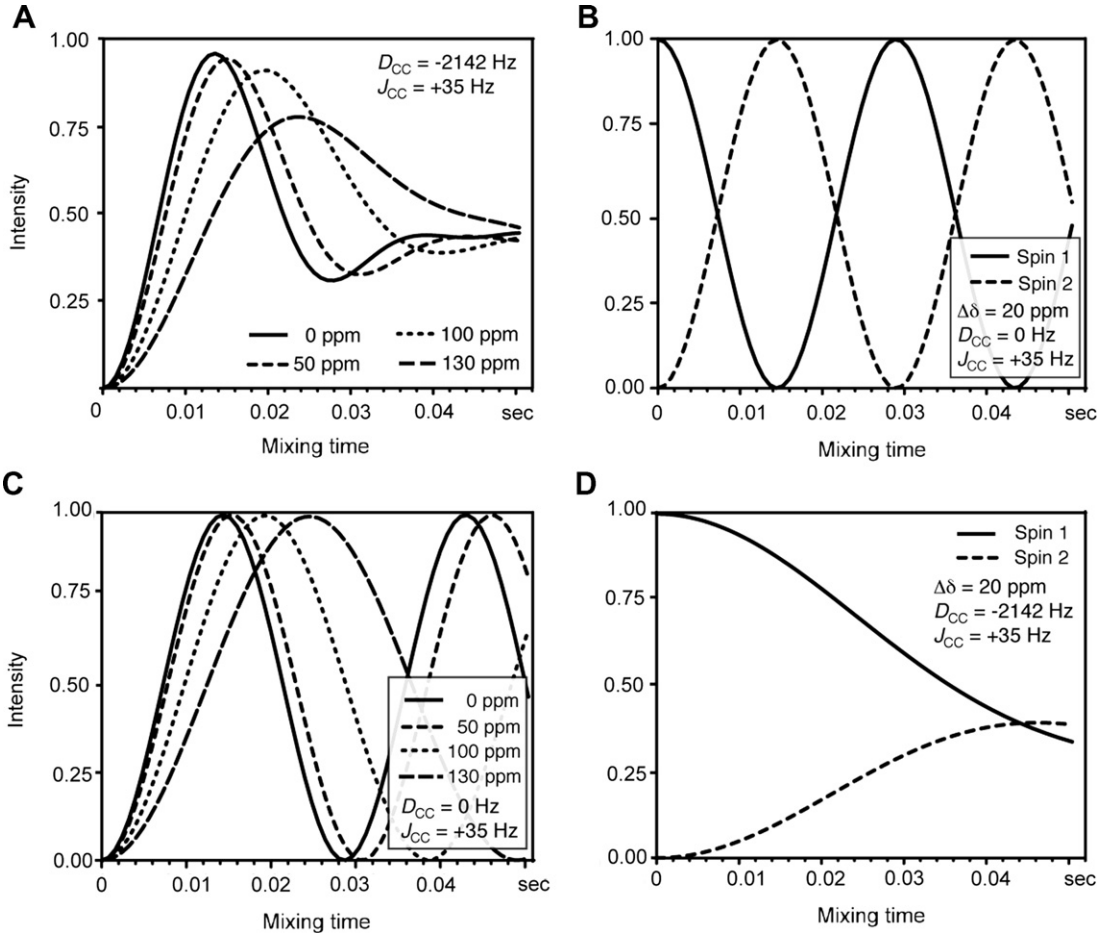

Fig. 5. Simulated magnetization transfer characteristics, assuming a two-spin system with longitudinal magnetization on spin 1 prior to mixing. The plots were generated using a 40 μs tanh pulse setting the MAS rotation frequency to 20 kHz. The experimentally employed shape was used as numerical input in the simulation. Similar as in the experimental implementation, a p5m4 phase cycle was employed in the simulation. $^{13}C,^{13}C$ scalar and dipolar couplings were assumed to be $^1J_{CC}$ = 35 Hz and D_{CC} = −2142 Hz, respectively. (A) Magnetization build up on spin 2 as a function of the chemical shift differences (indicated in the figure) in presence of D_{CC} and $^1J_{CC}$. (B) as (A), setting $\Delta\delta$ = 20 ppm and D_{CC} = 0. (C) Chemical shift difference dependence of the magnetization buildup on spin 2, setting D_{CC} = 0. The employed chemical shift differences are indicated in the figure. (D) as (A), setting $\Delta\delta$ = 20 ppm, $^1J_{CC}$ = 0 Hz and D_{CC} = −2142 Hz.

TOBSY sequence that we employ has a chemical shift offset dependence implying that the sequence introduces an additional error term into the Hamiltonian. The larger the chemical shift difference, the greater is the time that is required to transfer magnetization. Further, using a 20 ppm chemical shift difference (for which the offset dependence is negligible), the transfer characteristics of the sequence are evaluated in the absence of dipolar coupling. The transfer properties between the two spins (Fig. 5B) is purely scalar in nature. The first maximum in intensity occurs at $1/(2\,{}^{1}J_{CC})$, with complete magnetization transfer to the second spin. If

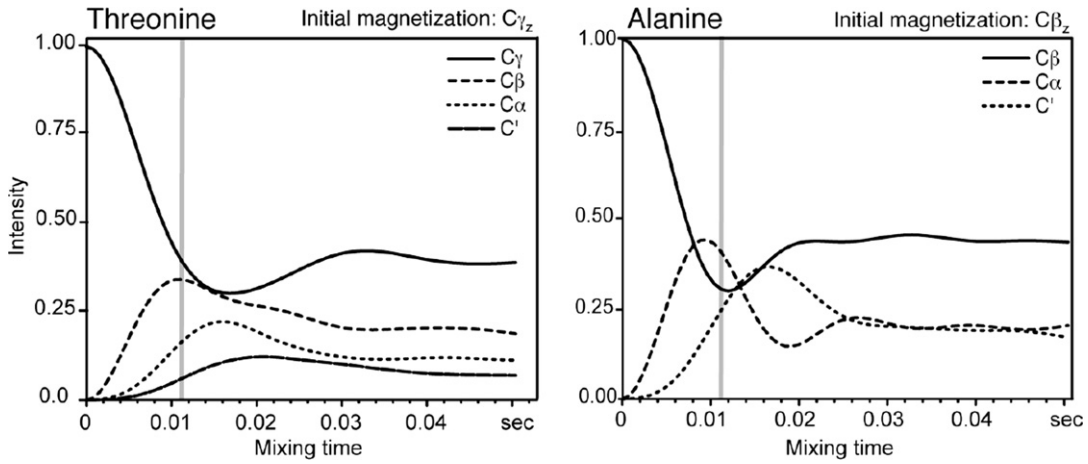

Fig. 6. Simulated magnetization build up for threonine and alanine. Only methyl carbons (Cγ for threonine, Cβ in case of alanine) are polarized at $t = 0$. All other parameters are the same as mentioned in the caption of Fig. 5. The gray shaded line at 11.2 ms represents the employed mixing time in the experiments applied to the α-spectrin SH3 domain.

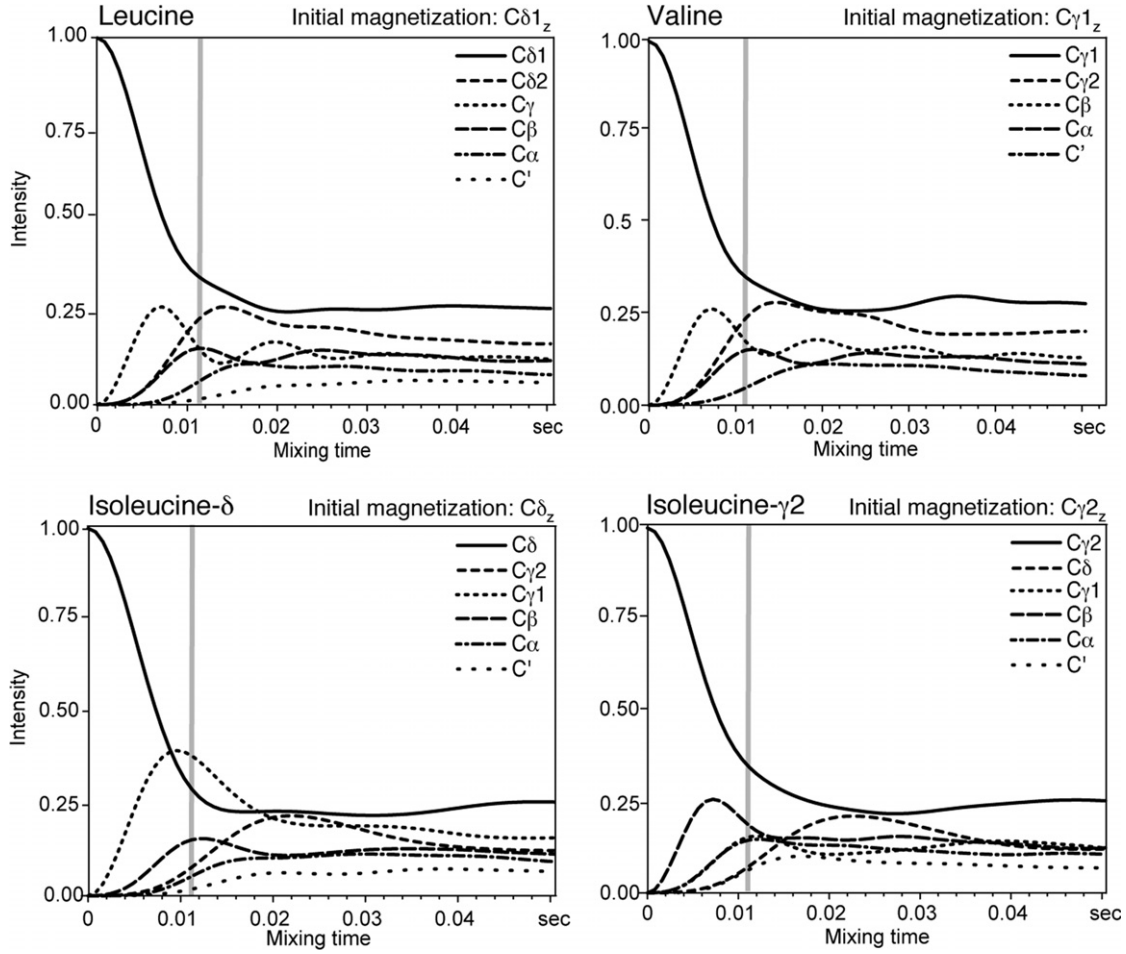

Fig. 7. Simulated magnetization build up for leucine, valine and isoleucine. Only methyl carbons (Cδ1 in leucine, Cγ1 in valine, Cδ and Cγ2 in isoleucine) are polarized at $t = 0$. All other parameters are the same as indicated in the caption of Fig. 5. The gray shaded line at 11.2 ms represents the employed mixing time in the experiments applied to the α-spectrin SH3 domain.

the chemical shift difference between the two spins is increased (Fig. 5C), the sequence is no more ideal, even in the absence of dipolar couplings. The first maximum gradually shifts to larger mixing times. It is noteworthy that still complete magnetization transfer occurs. In the other extreme, when two spins are only dipolar, but not scalar coupled, magnetization still exchanges between the two spins. However, the rate of transfer is very slow. Approximately 45% of magnetization is transferred from spin 1 to spin 2 after a mixing time of 50 ms. It is obvious that the sequence shows predominantly scalar transfer characteristics for short and medium mixing times. At longer mixing times the dipolar contribution becomes important.

Definition of the spin system in SIMMOL

In order to simulate the transfer characteristics of methyl bearing amino acids under TOBSY mixing, we employ the SIMMOL simulation program [46]. SIMMOL is employed to define the spin system (spinsys section) of the SIMPSON input file. Detailed information on how to generate a SIMPSON input (*spinsys*) is given in reference [46]. In brief, SIMMOL uses pdb files to calculate dipolar couplings from atomic coordinates. Isotropic shifts were used from the BMRB data base, while CSA and asymmetry parameters of individual amino acids are taken from reference [47]. A standard one-bond scalar coupling of 55 Hz was used for the interaction between Cα and C′, while for all other carbons $^1J_{CC}$ of 35 Hz was employed. Using this procedure, we extracted the *spinsys* input parameters for alanine, threonine, valine, leucine and isoleucine. All short and long range dipolar interactions were considered in the simulation.

Transfer characteristics of linear side chains (Ala and Thr)

Alanine and threonine represent linear three and four spin systems. Sequential build up of magnetization occurs on different carbons based on the number of bonds that are in between them and the methyl group. For alanine, the simulation shows that at a mixing time of 11.2 ms all correlation should be observable (Fig. 6). For threonine, only the correlations to CO are low in intensity (6–7% at 11.2 ms).

Transfer characteristics of branched side chains (Val, Leu and Ile)

Valine, leucine and isoleucine are branched side chains. The two methyl groups in valine and leucine are symmetric, hence the transfer characteristics are identical [48]. Cγ in leucine, Cβ in valine and isoleucine have multiple coupling partners. Therefore, maxima for magnetization transfer for those carbons occurs at mixing times of around 7–8 ms (Fig. 7). At longer mixing times (12–14 ms), the transfer is maximum for carbons separated by two bonds from the methyl position. The simulation shows that for a mixing time of 11.2 ms, two bond correlations should be observed, while one bond correlations to Cβ/Cγ in case of valine/leucine should be low in intensity. Isoleucine Cδ and Cγ1 show a two spin transfer characteristics. More than 40% of the magnetization is transferred from Cδ to Cγ1. Cβ is polarized via one bond from Cγ2 at short mixing times with a maximum intensity of 25%, while transfer to other carbons is extremely low even at long mixing time. The simulation for isoleucine shows why we only observe certain correlations in our experiment. The initial transfer profile is predominantly scalar in nature. At longer mixing time, the dipolar contribution becomes more important and the profile represents a superposition of both scalar and dipolar transfers. Our simulations show that at a mixing time of 11.2 ms experimentally all cross peaks are observed which have an intensity of greater than 0.2.

Fig. 8 shows that there is good match between experiment and simulation. In the experiment (Fig. 1), t_1 was incremented in the indirect dimension. The experiments are carried out using the triply labeled peptide NAc-Val-Leu-OH (approximately 1.5–2.0 mg of peptide was used for the experiment). Valine methyl protons are overlapped, whereas leucine methyl protons are spectrally re-

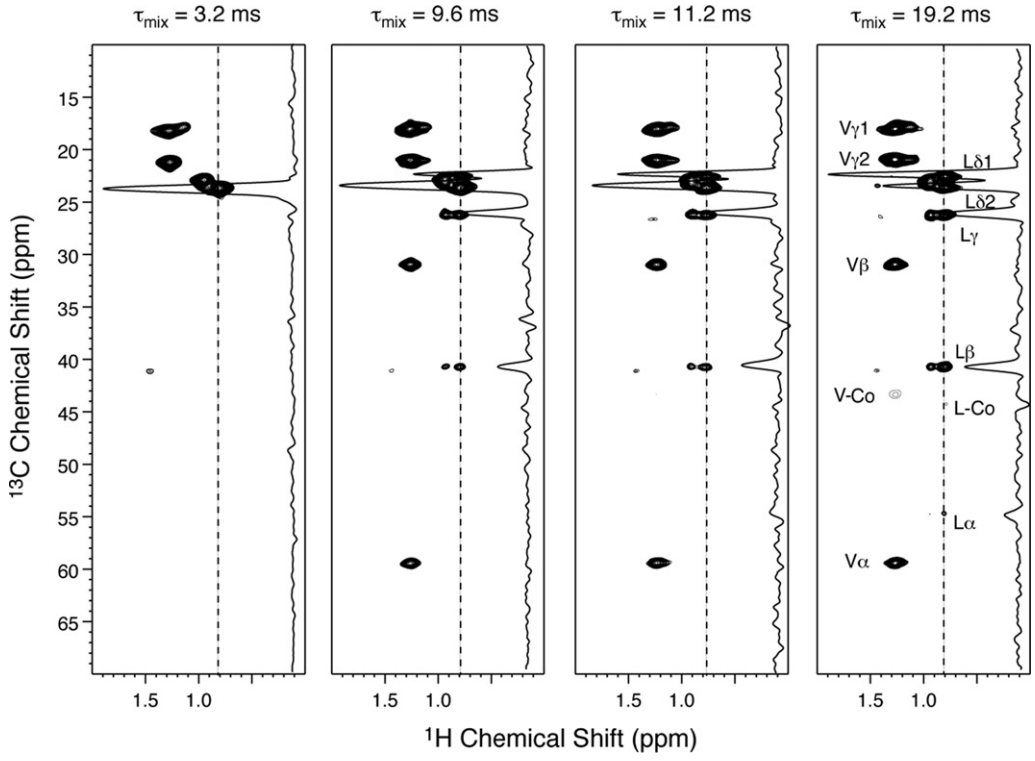

Fig. 8. 2D ^{1}H,^{13}C correlation evolving (f_1, f_3) pulse sequence shown in Fig. 1 employing TOBSY mixing times τ_{mix} of 3.2, 9.6, 11.2 and 19.2 ms. The triply labeled peptide NAc-Val-Leu-OH was used to demonstrate the experiments. 1D spectra along the ^{13}C dimension represent cross sections across one of the leucine resonances. Clearly, all correlations are observable at long TOBSY mixing times, however, with reduced sensitivity. The experimental time for each of the experiments amounted to approx. 7 h.

solved. The dashed line in the figure indicates the cross section along the carbon dimension of the 2D experiment which is represented as a 1D spectrum.

References

[1] M. Ernst, M.A. Meier, T. Tuherm, A. Samoson, B.H. Meier, Low-power high-resolution solid-state NMR of peptides and proteins, J. Am. Chem. Soc. 126 (2004) 4764–4765.

[2] A. Samoson, T. Tuherm, J. Past, A. Reinhold, T. Anupold, N. Heinmaa, New horizons for magic-angle spinning NMR, Top. Curr. Chem. 246 (2005) 15–31.

[3] D.H. Zhou, G. Shah, M. Cormos, C. Mullen, D. Sandoz, C.M. Rienstra, Proton-detected solid-state NMR spectroscopy of fully protonated proteins at 40 kHz magic-angle spinning, J. Am. Chem. Soc. 129 (2007) 11791–11801.

[4] A. Bielecki, A.C. Kolbert, M.H. Levitt, Frequency-switched pulse sequences—Homonuclear decoupling and dilute spin NMR in solids, Chem. Phys. Lett. 155 (1989) 341–346.

[5] E. Vinogradov, P.K. Madhu, S. Vega, High-resolution proton solid-state NMR spectroscopy by phase-modulated Lee-Goldburg experiment, Chem. Phys. Lett. 314 (1999) 443–450.

[6] E. Vinogradov, P.K. Madhu, S. Vega, Proton spectroscopy in solid state nuclear magnetic resonance with windowed phase modulated Lee-Goldburg decoupling sequences, Chem. Phys. Lett. 354 (2002) 193–202.

[7] A. Lesage, D. Sakellariou, S. Hediger, B. Elena, P. Charmont, S. Steuernagel, L. Emsley, Experimental aspects of proton NMR spectroscopy in solids using phase-modulated homonuclear dipolar decoupling, J. Magn. Res. 163 (2003) 105–113.

[8] L. Bosman, P.K. Madhu, S. Vega, E. Vinogradov, Improvement of homonuclear dipolar decoupling sequences in solid-state nuclear magnetic resonance utilising radiofrequency imperfections, J. Magn. Reson. 169 (2004) 39–48.

[9] B. Reif, C.P. Jaroniec, C.M. Rienstra, M. Hohwy, R.G. Griffin, ^{1}H–^{1}H MAS correlation spectroscopy and distance measurements in a deuterated peptide, J. Magn. Reson. 151 (2001) 320–327.

[10] B. Reif, R.G. Griffin, ^{1}H detected ^{1}H,^{15}N correlation spectroscopy in rotating solids, J. Magn. Reson. 160 (2003) 78–83.

[11] V. Chevelkov, B.J. van Rossum, F. Castellani, K. Rehbein, A. Diehl, M. Hohwy, S. Steuernagel, F. Engelke, H. Oschkinat, B. Reif, 1H detection in MAS solid state NMR spectroscopy employing pulsed field gradients for residual solvent suppression, J. Am. Chem. Soc. 125 (2003) 7788–7789.

[12] E.K. Paulson, C.R. Morcombe, V. Gaponenko, B. Dancheck, R.A. Byrd, K.W. Zilm, High-sensitivity observation of dipolar exchange and NOEs between exchangeable protons in proteins by 3D solid-state NMR spectroscopy, J. Am. Chem. Soc. 125 (2003) 14222–14223.

[13] E.K. Paulson, C.R. Morcombe, V. Gaponenko, B. Dancheck, R.A. Byrd, K.W. Zilm, Sensitive high resolution inverse detection NMR spectroscopy of proteins in the solid state, J. Am. Chem. Soc. 125 (2003) 15831–15836.

[14] C.R. Morcombe, E.K. Paulson, V. Gaponenko, R.A. Byrd, K.W. Zilm, H-1–N-15 correlation spectroscopy of nanocrystalline proteins, J. Biomol. NMR 31 (2005) 217–230.

[15] D.H. Zhou, J.J. Shea, A.J. Nieuwkoop, W.T. Franks, B.J. Wylie, C. Mullen, D. Sandoz, C.M. Rienstra, Solid-state protein-structure determination with proton-detected triple-resonance 3D magic-angle-spinning NMR spectroscopy, Angew. Chem. Int. Ed. 46 (2007) 8380–8383.

[16] V. Chevelkov, K. Rehbein, A. Diehl, B. Reif, Ultra-high resolution in proton solid-state NMR at high levels of deuteration, Angew. Chem. Int. Ed. 45 (2006) 3878–3881.

[17] M. Hologne, V. Chevelkov, B. Reif, Deuteration of peptides and proteins in MAS solid-state NMR, Prog. NMR Spect. 48 (2006) 211–232.

[18] R. Linser, V. Chevelkov, A. Diehl, B. Reif, Sensitivity enhancement using paramagnetic relaxation in MAS solid state NMR of perdeuterated proteins, J. Magn. Reson. 189 (2007) 209–216.

[19] V. Chevelkov, A. Diehl, B. Reif, Measurement of ^{15}N-T_1 relaxation rates in a perdeuterated protein by MAS solid-state NMR spectroscopy, J. Chem. Phys. 128 (2008) 052316.

[20] V. Chevelkov, K. Faelber, A. Schrey, K. Rehbein, A. Diehl, B. Reif, Differential line broadening in MAS solid-state NMR due to dynamic interference, J. Am. Chem. Soc. 129 (2007) 10195–10200.

[21] V. Chevelkov, A. Diehl, B. Reif, Quantitative measurement of differential 15N-Hα/β T2 relaxation times in a perdeuterated protein by MAS solid-state NMR spectroscopy, Magn. Res. Chem. 45 (2007) S156–S160.

[22] M. Hologne, K. Faelber, A. Diehl, B. Reif, Characterization of dynamics of perdeuterated proteins by MAS solid-state NMR, J. Am. Chem. Soc. 127 (2005) 11208–11209.

[23] M. Hologne, Z. Chen, B. Reif, Characterization of dynamic processes using deuterium in uniformly 2H,13C,15N enriched peptides by MAS solid-state NMR, J. Magn. Res. 179 (2006) 20–28.

[24] B. Reif, Y. Xue, V. Agarwal, M.S. Pavlova, M. Hologne, A. Diehl, Y.E. Ryabov, N.R. Skrynnikov, Protein side-chain dynamics observed by solution- and solid-state NMR: comparative analysis of methyl ^{2}H relaxation data, J. Am. Chem. Soc. 128 (2006) 12354–12355.

[25] V. Chevelkov, A.V. Zhuravleva, Y. Xue, B. Reif, N.R. Skrynnikov, Combined analysis of 15N relaxation data from solid- and solution-state NMR spectroscopy, J. Am. Chem. Soc. 129 (2007) 12594–12595.

[26] R. Lichtenecker, M.L. Ludwiczek, W. Schmid, R. Konrat, Simplification of protein NOESY spectra using bioorganic precursor synthesis and NMR spectral editing, J. Am. Chem. Soc. 126 (2004) 5348–5349.

[27] V. Agarwal, A. Diehl, N. Skrynnikov, B. Reif, High resolution ^{1}H detected ^{1}H,^{13}C correlation spectra in MAS solid-state NMR using deuterated proteins with selective ^{1}H,^{2}H isotopic labeling of methyl groups, J. Am. Chem. Soc. 128 (2006) 12620–12621.

[28] J. Leppert, O. Ohlenschlager, M. Gorlach, R. Ramachandran, Adiabatic TOBSY in rotating solids, J. Biomol. NMR 29 (2004) 167–173.

[29] R. Tycko, A. Pines, J. Guckenheimer, Fixed point theory of iterative excitation schemes in NMR, J. Chem. Phys. 83 (1985) 2775–2802.

[30] E.H. Hardy, R. Verel, B.H. Meier, Fast MAS total through-bond correlation spectroscopy, J. Magn. Reson. 148 (2001) 459–464.

[31] A. Detken, E.H. Hardy, M. Ernst, M. Kainosho, T. Kawakami, S. Aimoto, B.H. Meier, Methods for sequential resonance assignment in solid, uniformly C-13, N-15 labelled peptides: quantification and application to antamanide, J. Biomol. NMR 20 (2001) 203–221.

[32] E.H. Hardy, A. Detken, B.H. Meier, Fast-MAS total through-bond correlation spectroscopy using adiabatic pulses, J. Magn. Reson. 165 (2003) 208–218.

[33] T.D. Goddard, D.G. Kneller, SPARKY 3, University of California, San Francisco, 1997.

[34] D.M. LeMaster, Deuteration in protein proton magnetic resonance, Methods Enzymol. 177 (1989) 23–43.

[35] K.H. Gardner, L.E. Kay, The use of H-2, C-13, N-15 multidimensional NMR to study the structure and dynamics of proteins, Annu. Rev. Biophys. Biomol. Struct. 27 (1998) 357–406.

[36] V.C. Phan, E.A. Fry, L.A. Crum, E.K. Paulson, C.R. Morcombe, J. Hans, R.A. Byrd, K.W. Zilm. Spin Exchange and Cross Relaxation in the Solid State NMR of Proteins, April 22–27, 2007, Daytona Beach, Florida, USA.

[37] O.C. Andronesi, S. Becker, K. Seidel, H. Heise, H.S. Young, M. Baldus, Determination of membrane protein structure and dynamics by magic-angle-spinning solid-state NMR spectroscopy, J. Am. Chem. Soc. 127 (2005) 12965–12974.

[38] A.B. Siemer, A.A. Arnold, C. Ritter, T. Westfeld, M. Ernst, R. Riek, B.H. Meier, Observation of highly flexible residues in amyloid fibrils of the HET-s prion, J. Am. Chem. Soc. 128 (2006) 13224–13228.

[39] A. Bax, G.M. Clore, A.M. Gronenborn, H-1–H-1 correlation via isotropic mixing of C-13 magnetization, a new 3-dimensional approach for assigning H-1 and C-13 spectra of C-13-enriched proteins, J. Magn. Reson. 88 (1990) 425–431.

[40] V. Tugarinov, L.E. Kay, Ile, Leu, and Val methyl assignments of the 723-residue malate synthase G using a new labeling strategy and novel NMR methods, J. Am. Chem. Soc. 125 (2003) 13868–13878.

[41] V. Tugarinov, L.E. Kay, Side chain assignments of Ile delta 1 methyl groups in high molecular weight proteins: an application to a 46 ns tumbling molecule, J. Am. Chem. Soc. 125 (2003) 5701–5706.

[42] L.L. Chen, R.A. Olsen, D.W. Elliott, J.M. Boettcher, D.H.H. Zhou, C.M. Rienstra, L.J. Mueller, Constant-time through-bond C-13 correlation spectroscopy for assigning protein resonances with solid-state NMR spectroscopy, J. Am. Chem. Soc. 128 (2006) 9992–9993.

[43] L. Chen, J.M. Kaiser, T. Polenova, J. Yang, C.M. Rienstra, L.J. Mueller, Backbone assignments in solid-state proteins using J-based 3D heteronuclear correlation spectroscopy, J. Am. Chem. Soc. 129 (2007) 10650–10651.

[44] M. Bak, J.T. Rasmussen, N.C. Nielsen, SIMPSON: a general simulation program for solid-state NMR spectroscopy, J. Magn. Reson. 147 (2000) 296–330.

[45] M. Baldus, D.G. Geurts, S. Hediger, B.H. Meier, Efficient N-15-C-13 polarization transfer by adiabatic-passage Hartmann–Hahn cross polarization, J. Magn. Reson. A 118 (1996) 140–144.

[46] M. Bak, R. Schultz, T. Vosegaard, N.C. Nielsen, Specification and visualization of anisotropic interaction tensors in polypeptides and numerical simulations in biological solid-state NMR, J. Magn. Reson. 154 (2002) 28–45.

[47] C.H. Ye, R.Q. Fu, J.Z. Hu, L. Hou, S.W. Ding, C-13 chemical-shift anisotropies of solid amino-acids, Magn. Res. Chem. 31 (1993) 699–704.

[48] H.L. Eaton, S.W. Fesik, S.J. Glaser, G.P. Drobny, Time-dependence of C-13–C-13 magnetization transfer in isotropic mixing experiments involving amino-acid spin systems, J. Magn. Reson. 90 (1990) 452–463.